

Oxygen-induced Rh $3d_{5/2}$ surface core-level shifts on Rh(111)

M. V. Ganduglia-Pirovano,¹ M. Scheffler,¹ A. Baraldi,² S. Lizzit,² G. Comelli,^{3,4} G. Paolucci,² and R. Rosei^{3,4}

¹*Fritz-Haber-Institut der Max-Planck-Gesellschaft, Faradayweg 4-6, D-14 195 Berlin-Dahlem, Germany*

²*Sincrotrone Trieste S.C.p.A., S.S. 14 Km 163.5, 34012 Basovizza, Trieste, Italy*

³*Dipartimento di Fisica, Universita' di Trieste, 34127 Trieste, Italy*

⁴*Laboratorio T.A.S.C.-I.N.F.M., S.S. 14 Km 163.5, 34012 Basovizza, Trieste, Italy*

(Received 8 November 2000; published 1 May 2001)

High-resolution measurements are reported of the surface core-level shift (SCLS) of the $3d$ level for the Rh(111) surface as a function of oxygen coverage Θ on the surface. These measurements are analyzed by density-functional theory calculations of the initial- and final-state contributions to the shifts. The calculations are found to reproduce well the trends and magnitudes of the experimental shifts. Adsorption of oxygen shifts the Rh $3d$ surface core levels to higher binding energies with the magnitude of the shift depending almost linearly on the coordination number of Rh surface atoms to O adatoms. The Rh $3d$ binding energy increases by about 0.3 eV per bond to an O adatom. This correlation is robust with respect to differences between initial- and transition-state theory calculations of the SCLS's. The results are discussed in a simple physical picture.

DOI: 10.1103/PhysRevB.63.205415

PACS number(s): 73.20.At, 71.20.Be, 79.60.-i

I. INTRODUCTION

Oxygen adsorption on metal surfaces can result in simple adsorbate-covered surfaces, subsurface oxygen penetration, or oxide formation, depending on the oxygen partial pressure, substrate temperature, surface crystallographic orientation of the particular metal, and the time of exposure. Over recent years, several experimental studies under ultra-high-vacuum (UHV) conditions and low temperatures on the surface crystal structure of low coverage phases of chemisorbed oxygen on Rh(111) have been reported, using primarily low-energy electron diffraction (LEED), scanning tunnel microscopy (STM), and x-ray photoelectron diffraction (XPD).¹⁻⁹ Theoretical work using density-functional theory (DFT) calculations has also been recently reported, predicting that an O adlayer with a (1×1) periodicity and coverage $\Theta = 1.0$ monolayer (ML) can form on Rh(111).^{10,11} This result differs markedly from the half coverage (2×1) adlayer structure which forms at saturation when using molecular oxygen at room temperature and UHV conditions. Recently, it has been experimentally confirmed that indeed a full monolayer of chemisorbed O can be prepared at room temperature on Rh(111) by using an atomic O beam.¹² Moreover, we note that it is possible to deposit more than 0.5 ML of O with long O₂ exposure of the Rh(111) surface at elevated surface temperatures and that the formation of subsurface oxygen species has been observed, when the 1.0-ML oxygen adlayer is nearly completed.¹³ The *qualitative* difference between a high-coverage oxygen adsorbate phase, namely a high coverage on the surface plus subsurface oxygen, and an oxidized Rh(111) surface is unclear. Thus the knowledge of the nature of the oxygen-metal interaction spanning the range from low to high temperatures and pressures is as yet incomplete. In this context it is of particular importance to identify and characterize the intrinsic similarities and differences of the O-metal bonding in different chemical environments.

In order to examine this point, we have studied both experimentally and theoretically the oxygen induced Rh $3d$ surface core-level shifts (SCLS's), defined as the core-level

binding energy difference between the Rh atoms at the surface and in the bulk,¹⁴ for the Rh(111) surface as a function of oxygen coverage on the surface. The SCLS's are related to differences in the electronic and geometrical structures of the atoms in the first and in deeper layers of a solid, and are influenced by different adsorbate-substrate environments. Additionally, the core levels of chemisorbed atoms and molecules are very sensitive to the adsorption site.¹⁵⁻¹⁸ We have also studied the O $1s$ core-level shift (CLS) relative to the lowest coverage structure at a coverage $\Theta = 0.25$ ML. Since our aim is to understand the changes in the nature of the O-metal interaction all the way from adlayers to surface oxides, the present study was undertaken as a first step to specifically demonstrate how core-level shifts reflect the adsorbate geometrical and electronic structures of the O adlayers.

From the experimental point of view the determination of SCLS for the $3d_{5/2}$ core levels of $4d$ transition metals requires high-energy resolution photoemission measurements with synchrotron radiation. The large lifetimes of these core holes imply very narrow photoemission peaks, and the variations in the position of the core-level induced by atomic and/or molecular adsorption are very small. Moreover, a high surface sensitivity, obtained by tuning the photon energy, is needed in order to detect the surface components.

Theoretically SCLS's are very often interpreted in terms of the initial-state picture, i.e., the difference of the single-particle energy eigenvalues of a surface and a bulk atom core state. This approach neglects the possibility of a different response of the valence electrons at the surface and in the bulk to the created core hole. That this difference, i.e., the final-state effect, can make a substantial contribution to the shifts was shown in Refs. 19 and 20 for clean surfaces and in Ref. 21 for metallic surface alloys on metal substrates.

In the present work we have performed density-functional theory calculations including both the initial- and final-state contributions to the shifts, thus allowing for an unambiguous separation of these effects and an estimate of their relative importance. These calculations are found to reproduce well the trends and magnitudes of the experimental shifts and are

used to discuss the origin of the different contributions to the measured shifts. We find that the negative initial-state contribution to the Rh $3d$ SCLS of the clean Rh(111) surface is reduced and then becomes positive upon oxygen chemisorption with increasing coverage. To a certain degree this reflects the electronegativity of the oxygen adatoms. We examine the relation between the shift of the Kohn-Sham potential at the surface relative to the bulk, the initial-state surface $3d$ core-level shift and the displacement of the center of gravity of the surface $4d$ band, ΔC_d . We show that despite the complex spatial dependence of the changes in the self-consistent potential at the surface and the location of the $3d$ and $4d$ orbitals in different regions of space, a correlation between oxygen induced SCLS's and ΔC_d 's exists because the SCLS's and the ΔC_d 's arise from the adsorbate-induced shift of the Kohn-Sham potential experienced by the core states and the d states, respectively.

The self-consistent d -band structure is complex, with changes in width, shape, and center of gravity position at the surface. To gain more insight into the origin of the ΔC_d 's and the SCLS's, we have calculated the increase in the mean square width of the projected density of states per Rh surface atom onto the $4d$ orbitals (d DOS) upon oxygen chemisorption relative to the bulk d DOS's. By mapping the self-consistent d DOS's onto rectangular model d bands with similar relative changes of the mean-square width as those of the actual self-consistent d DOS's, and assuming *strict* conservation of d charge for each layer, we have calculated the displacement of the center of gravity of the model surface d -band (relative to the bulk) $\Delta C_d^{\text{model}}$, which arises from the change in the surface d -band width. In agreement with findings for O/Ru(0001),^{22,23} we find that the resulting $\Delta C_d^{\text{model}}$ trend correlates with the calculated SCLS's initial-state trend and that layerwise d -charge conservation holds approximately.

Inclusion of final-state effects are important for accurate calculations of SCLS's and reveals that the screening of the $3d$ core hole, which is more effective for a surface than for a bulk atom for the clean Rh(111) surface,²⁰ becomes less effective at higher O coverages. This behavior is understood in terms of the oxygen induced changes in the Rh surface $4d$ band, in which the screening occurs, and the consequent lowering of the density of states at and close to the Fermi level.

As the oxygen coverage increases the distance between partially negatively charged O adatoms decreases and a repulsive adsorbate-adsorbate interaction builds up, which leads to the decreased adsorption energy with increasing coverage.¹¹ Partially reducing the electron transfer and the oxygen induced dipole moment per adatom is energetically favorable for higher coverages as it reduces the O-O repulsion. A positive initial-state O $1s$ shift of the $p(1\times 1)$ -O structure ($\Theta = 1.0$ ML) with respect to the $p(2\times 2)$ -O structure ($\Theta = 0.25$ ML) and the saturation of the work function change as function of coverage at ($\Theta \approx 0.75$ ML) reflect that effect.

The paper is structured in the following way. After a short description of the experimental technique (Sec. II), the details of the calculation of the initial- and final-state contributions to the shifts will be described (Sec. III). In Sec. IV we

present and discuss the experimental and theoretical results. Here the evolution and decomposition of the Rh $3d_{5/2}$ spectra when O is adsorbed are described, and the validity of the assignment of the peaks is discussed while comparing measured and calculated values for the shifts. Finally, we explain the trends observed for the initial- and final-state contributions. In Sec. V our results and conclusions are summarized.

II. EXPERIMENTAL

The high-resolution core-level photoemission experiments have been carried out at the SuperESCA beamline of ELETTRA, which is the third generation synchrotron light source placed in Trieste, Italy.^{24,25} The third generation synchrotron light source placed in Trieste, Italy. The chamber was equipped with a VSW 150-mm 16 parallel channels hemispherical electron energy analyzer operated with a pass energy of 5 and 20 eV for the Rh $3d_{5/2}$ and O $1s$ core-level measurements, respectively. The monochromator energy resolution was varied from 60 to 200 meV, corresponding to a total instrumental resolution in the range of 60–240 meV, depending on photon energy (390 and 650 eV). LEED was used to detect the $p(2\times 2)$ and $p(2\times 1)$ long-range ordered structures formed upon oxygen adsorption on the surface at room temperature. The ambient background pressure in the chamber was 8×10^{-11} mbar, dominated by hydrogen. The Rh(111) sample used in the experiments was oriented within 1° and mechanically polished. The following procedure was used for sample cleaning. Initially the surface was cleaned using Ar⁺ sputtering at room temperature, annealing at 1300–1350 K, and oxygen treatments at 800–1100 K in order to remove the carbon. Hydrogen reduction at 400–700 K was then used to remove the oxygen. The surface temperature was monitored using two K-type thermocouples spot welded to the sides of the crystal and controlled using a Eurotherm programmable temperature device. Oxygen gas of 99.999 purity was used in the experiments. We want to point out that the saturation coverage for O₂ exposure below 50 Langmuir at room temperature results to be 0.5 ML, while a (1×1) oxygen overlayer at 1.0 ML can be obtained on Rh(111) only by dosing NO₂ or atomic oxygen.¹² Rh $3d_{5/2}$ and O $1s$ core-level spectra binding energies have been calibrated with respect to the Fermi energy.

III. THEORETICAL

In exact terms, the measured surface core level shift Δ_c is the difference in the energy that it takes to remove one electron from a core state of surface and a bulk atom. Each ionization energy is itself a difference of two total energies, namely, those before and after the core electron is removed. To a good approximation, this difference can also be obtained via the Slater-Janak transition-state approach to evaluate total-energy differences.²⁶ The total energy is a function of the core-level occupation which can be taken as a continuous variable. The initial-state theory is the first-order term in the expansion of these total energies into Taylor series in the change of the core occupation, whereas the transition state theory includes the terms up to second order. Then the full

calculated shift Δ_c is given by

$$\Delta_c \approx -[\epsilon_c^{\text{surf}}(n_c - 1/2) - \epsilon_c^{\text{bulk}}(n_c - 1/2)]. \quad (1)$$

ϵ_c^{surf} and ϵ_c^{bulk} denote the Kohn-Sham eigenvalues of a particular core state of a surface or bulk atom, and n_c is the occupation number. In the initial-state approximation, the SCLS is exactly given by Eq. (1) with occupation n_c .

The electron density, surface atomic structure, total energies, and core-electron eigenvalues are calculated using density-functional theory and the generalized gradient approximation (GGA) of Perdew *et al.*²⁷ for the exchange-correlation functional as implemented in the all-electron full-potential linear augmented plane-wave method (FP-LAPW).^{28–30} The Rh(111) surface is modeled using a supercell approach, where we use a seven layer (111) Rh slab with a vacuum region corresponding to six interlayer spacings. Oxygen atoms are adsorbed on both sides of the slab. Oxygen atoms and all atoms in the two outer Rh substrate layers are allowed to relax while the central three layers of the slab were fixed in their calculated bulk positions. Details of the calculations and the optimized geometries have been described elsewhere.¹¹ Calculations have been performed for the $p(2 \times 2)$, $p(2 \times 1)$, and (1×1) -O phases which correspond to coverages $\Theta = 0.25, 0.5$, and 1.0 ML, respectively. The calculated atomic geometries (interlayer spacings, bond lengths, and lateral displacements) at 0.25 and 0.5 ML (see Ref. 11) are in excellent agreement with the results of previous LEED I-V analyses.^{5,6}

To describe the transition state [see Eq. (1)], we performed self-consistent electronic structure calculations for an impurity, i.e., an atom with half an electron missing in the particular core level. We used (2×2) supercells in the surface plane, in order to have the ionized atom surrounded by nonionized nearest-neighbor atoms. The geometry was not allowed to vary from the initial-state one and overall charge neutrality was imposed, i.e., half an electron was added at the Fermi level. This accounts for the Fermi reservoir of the substrate and describes to a good approximation an electronically relaxed final state. The calculated final-state or screening contributions to the shifts are given by the difference between the transition-state theory calculation and the calculated initial-state shifts. Calculations of the initial- and final-state contributions to the Rh $3d$ shifts were performed for the Rh atoms of the two outer Rh substrate layers. For the Rh bulk atoms, we considered those of the middle plane of an 11 layer (111) slab (with no vacuum region) in order to obtain the same sampling of the reciprocal space in all calculations.

To investigate the final-state contributions to the O $1s$ core-level binding-energy shifts, similar impurity calculations have been performed, i.e., self-consistent electronic structure calculations for an O atom with half an electron missing in the $1s$ level with a (2×2) periodicity. Shifts are referred to the lowest coverage structure at $\Theta = 0.25$ ML.

To test the accuracy of our calculated SCLS's on a number of numerical approximations, namely, the cutoff energy of the plane-waves basis set, the slab thickness, and the number of \mathbf{k} points to sample the Brillouin zone, selected calculations were repeated with more accuracy. We calculated the

SCLS's of the clean and the highest 1.0 -ML coverage (1×1) structure, which are the lower and upper bound of the coverage sequence considered. The present self-consistent structure optimizations and SCLSs calculations were conducted for a 16 -Ry cutoff and a $(12 \times 12 \times 1)$ Monkhorst-Pack grid for the (1×1) unit cell with 19 \mathbf{k} points in the irreducible wedge.¹¹ The changes in the calculated SCLSs due to a larger plane-waves cutoff of 24 Ry, as well as denser \mathbf{k} meshes up to a $(18 \times 18 \times 1)$ grid with 37 \mathbf{k} points in the irreducible wedge, were within ± 10 meV. Furthermore, extending the Rh(111) slab from 7 to 9 and 11 layers revealed changes in the SCLS's up to ± 10 meV. These tests show that the errors induced by these numerical approximations ($\sim \pm 20$ meV) are of the same order as the experimental error (see Sec. IV A). A similar estimation of the numerical accuracy has been given for O/Ru(0001) in Ref. 23.

IV. RESULTS AND DISCUSSION

A. Experimental

In this section, we describe the experimental results focusing in particular on how the SCLS's are extracted from the data. In Fig. 1 we show the Rh $3d_{5/2}$ core-level spectra for the clean Rh(111) surface, $p(2 \times 2)$ -O/Rh(111) ($\Theta = 0.25$ ML) and $p(2 \times 1)$ -O/Rh(111) ($\Theta = 0.5$ ML) ordered structures measured at 300 K. The clean spectrum exhibits two well resolved peaks: the lower binding energy peak is attributed to the Rh atoms of the first substrate layer while the higher binding energy component to atoms in the deeper layers, i.e., bulk layers. In order to evaluate quantitatively the surface core-level shifts, spectral decomposition into bulk and surface components has been performed by fitting the data using two peaks with Doniach-Sunjić (DS) line shape.³¹ The DS function, which is commonly used to fit the line shape of metallic core levels, is described by two parameters, the singularity index α (final-state screening of the core hole) and the Lorentzian width Γ (core-hole lifetime). The two DS peaks, which were allowed to have different α and Γ , were convoluted with Gaussians in order to account for the experimental, phonon, and inhomogeneous broadening. A linear background was also included into the fit. The result of the least-squares analysis is shown in Fig. 1 as a solid line through the measured points, and the single bulk and surface components are also shown. Within the accuracy of the analysis, the SCLS we find for the clean surface 485 ± 20 meV, as well as the values of the line-shape parameters, reported in the figure caption, are in good agreement with previous experimental findings by Andersen *et al.*³² The number of components used in the fits of the spectra at 0.25 and 0.5 ML has been decided on the basis of the known structural models.⁶ At 0.25 ML, the model proposed for the $p(2 \times 2)$ structure, displayed in Fig. 1, involves two inequivalent first substrate layer Rh atoms, one not bonded to oxygen adatoms (A) and one directly bonded to a single oxygen adatom (B). Only type-A atoms are present in the clean surface. The $p(2 \times 1)$ structure is also formed by two different types of surface Rh atoms (see Fig. 1): the first type is bonded to one oxygen adatom and in a first approximation can be considered as being in a similar chemical environ-

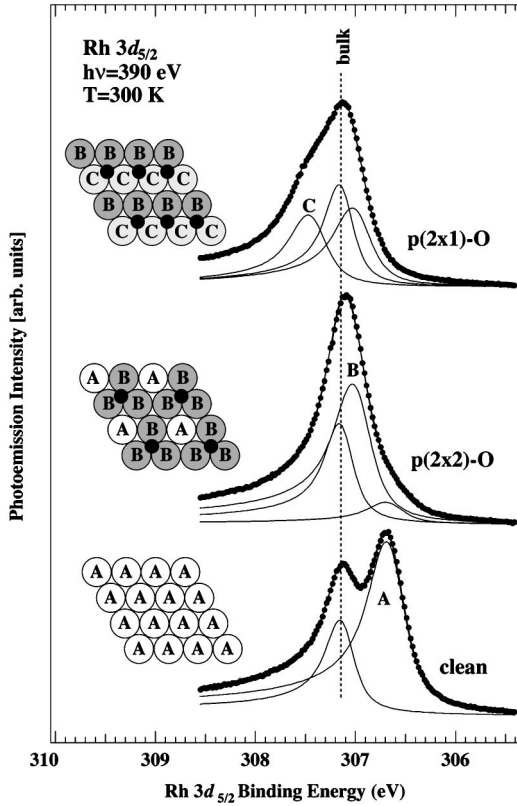


FIG. 1. Decomposition of Rh $3d_{5/2}$ core-level photoemission spectra of the clean Rh(111) surface and its evolution as a function of oxygen coverage into Doniach-Šunjić line shapes. Dots are experimental data and full lines are the total fitted spectrum. The individual surface and bulk components are also shown. A is the peak associated to Rh surface atoms which are not bound to oxygen. B and C are the peaks associated to Rh atoms coordinated to one or two O adatoms, respectively. Insets: Structural models for the two O-covered structures at 0.25 and 0.5 ML; small black circles, O adatoms. Fitting parameters are $\Gamma=0.22$ and 0.27 eV, $\alpha=0.19$ and 0.26 , and Gaussian broadenings = 0.22 and 0.26 for bulk and surface peaks, respectively.

ment as atoms B of the $p(2\times 2)$ structure; the second type (C) forms two bonds with oxygen adatoms. To each of these three Rh species (A, B, and C) we associated differently shifted core-level components in the fits. This interpretation is corroborated by the theoretical results presented in the next section. Such an assignment, based on the different adsorbate to metal atom coordination numbers has been previously made for the interpretation of measured SCLS's for the CO/Pd(110)³³ and O/Ru(10 $\bar{1}$ 0) systems.¹⁸ Best fits were obtained with a SCLS (measured respect to the bulk energy position) of -485 ± 20 , -140 ± 20 , and $+295\pm 20$ meV for the type-A, B, and C Rh atoms, respectively. Note that this classification contains a slight simplification because only the coordination of the Rh atoms considered is taken into account and possible differences in the local geometrical environment due to oxygen induced lateral and vertical displacements of Rh atoms in the outermost layers among the considered structures are ignored. However, the theoretical shifts discussed below indicate that the differences intro-

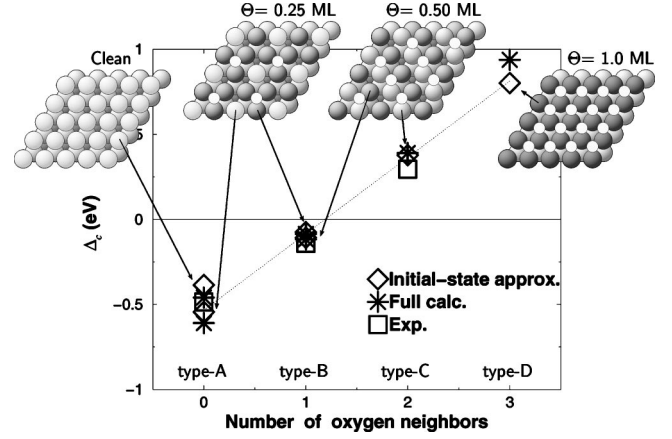


FIG. 2. Surface Rh $3d$ core-level shifts at the Rh(111) surface in the initial-state approximation and as obtained from the transition-state approach (containing final-state screening contributions to the shifts) as a function of the Rh surface atoms coordination to O adatoms. Insets: Structural models (small white circles are the O adatoms). Comparison between calculated and measured values is shown for the clean, $p(2\times 2)$ -O ($\Theta=0.25$ ML), and $p(2\times 1)$ -O ($\Theta=0.50$ ML) phases.

duced by these effects are small compared to those between a type-A, B, and C atoms. In principle, the intensity ratios of the different Rh components should correspond to the relative amounts of Rh atoms bonded to none, one, and two O adatoms, respectively, but photoelectron diffraction effects might in general affect the intensity of the different components. We have also measured the O $1s$ core levels corresponding to the 0.25- and 0.5-ML oxygen structures. Our data show that the $p(2\times 2)$ to $p(2\times 1)$ core-level shift is -110 ± 30 meV.

B. Theoretical

Let us now compare the experimental results to the calculated shifts. We will first consider the $3d$ shifts of Rh surface atoms, i.e., those of the outer substrate layer, then we will discuss the shifts of second substrate layer atoms. Finally, the results for the O $1s$ shifts will be compared.

Results for the Rh $3d$ initial-state SCLS's and from the transition-state theory calculation [see Eq. (1)] for atoms at the Rh(111) surface layer as a function of O coverage are shown in Fig. 2 and Table I. The final-state contributions to the shifts are displayed in Fig. 3. The calculated SCLS of the clean Rh(111) surface is -459 meV, thus in good agreement with the experimental value of -485 ± 20 meV. The screening contribution to this value is -74 meV. These values are in line with earlier measurements and DFT-LDA results for Rh(111) of -500 ± 20 meV and -420 meV, respectively.³² The fact that the initial-state SCLS is negative for Rh surfaces is qualitatively well understood and has been explained by using the narrower d band at the surface due to the reduced coordination number for the surface atoms relative to the bulk, and assuming an approximate conservation of d charge in each layer.^{17,20,34,35} Hence the self-consistent potential at the surface changes so as to maintain the d -band filling approximately constant, and consequently the surface

TABLE I. The Rh $3d$ surface core-level shifts (meV) at the (111) surface of Rh as obtained from the transition-state theory and from the initial-state model as a function of the O coordination or type, given in parentheses (see Fig. 2). The third column shows the difference and gives the screening or final-state contribution to the shifts.

Coverage	O coordination		Full calc.	Initial state	Final state
Clean	0	(A)	-459	-385	-74
0.25	0	(A)	-609	-544	-65
	1	(B)	-85	-75	-10
0.50	1	(B)	-116	-106	-10
	2	(C)	+391	+378	+13
1.00	3	(D)	+939	+801	+138

d band shifts relative to the bulk band. This perturbing potential acts on the core electrons as well and is repulsive for late transition metals, and attractive for early transition metals. The calculated screening contribution for Rh(111) is negative. Thus, when it is taken into account, the theoretical result comes in close agreement with the experimental data. A negative final-state contribution to the SCLS's means that the relaxation energy is larger for a surface than for a bulk atom, i.e., a core hole in a surface atom is better screened than one in a bulk atom. This enhanced screening at the surface is partially due to a better intra-atomic screening, i.e., screening provided by the high-lying localized d states at the atom from which the core electron was emitted.²⁰

1. Initial-state O-induced shifts

In order to understand the changes in the Rh $3d$ spectra upon oxygen adsorption, it is instructive to discuss first the trends of the core-electron eigenvalues of the nonexcited systems in their electronic ground states, i.e., the initial-state contributions to the Rh $3d$ shifts. The results presented in Fig. 2 and Table I clearly demonstrate that there is a strong

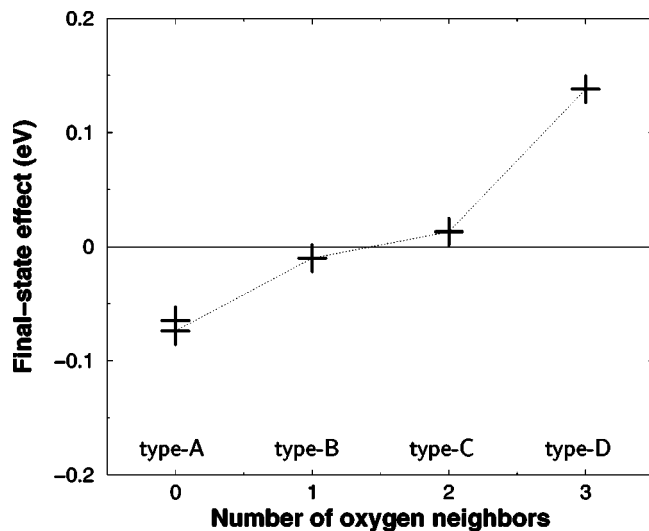


FIG. 3. Calculated final-state contribution to the Rh $3d$ SCLS's at the Rh(111) surface as a function of the Rh surface atoms coordination to O adatoms for the clean and O covered surfaces.

oxygen coverage dependence of the initial-state contribution to the SCLS's. The lowest energy structures at all coverages are phases with O adatoms at the fcc hollow sites.¹¹ Focusing on the Rh surface atoms it has been discussed in the previous section that the surface Rh layer at a coverage of 0.25 ML contains two inequivalent Rh atoms, namely those directly bonded to one O adatom (type B) and those not bonded to oxygen (type A). On the basis of the calculations, the difference in Rh $3d$ initial-state shifts of the clean Rh(111) surface and the type-A atoms of the $p(2 \times 2)$ -O/Rh(111) phase is ~ 160 meV (see Table I). We attribute this difference to oxygen-induced surface relaxations, which result in a slightly modified geometrical environment for the type-A Rh atoms of the $p(2 \times 2)$ -O/Rh(111) structure compared to that for surface atoms at the clean Rh(111) surface. LEED analyses and DFT-GGA calculations have shown that oxygen adsorption induces buckling and a substantial overall expansion of the first interlayer spacing.^{6,11} At a coverage of 0.25 ML the mean outermost Rh interlayer distance is calculated to be expanded by 0.04 Å, compared to the bulk interlayer spacing, i.e., 0.08 Å compared to the outermost interlayer spacing of the clean surface. The latter is contracted by 0.04 Å compared to the bulk value. The triangle formed by the three Rh atoms in the surface layer below the O adatom has laterally expanded by about 0.03 Å and the buckling in the surface layer is about 0.13 Å. The calculated 160-meV difference between both type-A Rh atoms reflect to a certain degree these changes in the crystal structure. However, this difference is small compared to that between type-A and type-B atoms. The calculated initial-state contribution to the SCLS's of type-B Rh atoms of the $p(2 \times 2)$ structure ($\Theta = 0.25$ ML) is -75 meV, i.e., $3d$ levels are 310 meV stronger bound relative to those of the clean surface atoms (see Table I).

The higher 0.50-ML coverage $p(2 \times 1)$ -O/Rh(111) structure also contains two kinds of inequivalent Rh atoms at the surface, which are coordinated either to one (type-B) or two (type-C) O adatoms (see Fig. 2). The calculated initial-state SCLS's are -106 and 378 meV, respectively. The shift -106 meV for the type-B atoms differs by 31 meV from that of those Rh atoms also coordinated to one O adatom in the 0.25-ML phase. The small difference reflects that the atoms are similar but not identical due to the slightly modified local geometries of the different types of atoms of the considered structures.¹¹ However, larger shifts towards higher binding energies are obtained for type-C atoms, which are completely absent in the 0.25 ML phase.

At the highest coverage of 1.0 ML there is only one kind of Rh site (type D), namely Rh atoms coordinated to three O adatoms. Core levels are shifted to even larger binding energies. The initial-state results given in Fig. 2 show a quasilinear correlation of the shifts and the number of O atoms to which the metal atom is coordinated. This initial-state trend, i.e., that the core levels are shifted towards higher binding energies as coverage increases, is precisely what is expected from the chemisorption of electronegative species on metal surfaces. Electron withdrawing O adatoms reduce electron-electron repulsion in the core of their Rh nearest neighbors and the potential at the surface changes relative to the bulk. This surface potential shift acts on both the surface valence d

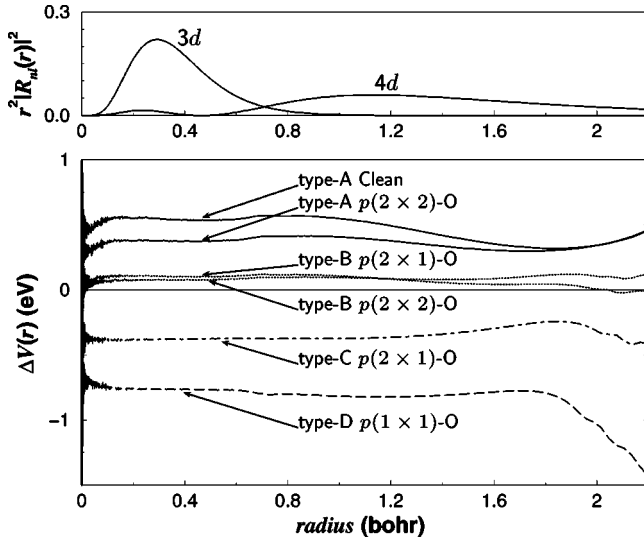


FIG. 4. Surface potential shift $\Delta V(r)$ for all surface Rh atoms at the coverages considered. Type-A atoms are not bound to oxygen. B, C, and D are Rh atoms coordinated to one, two, or three O adatoms, respectively. Radial solutions $r^2 |R_{nl}(r)|^2$, $nl = 3d$ and $4d$ within the muffin-tin sphere of 2.2 bohr in the bulk.

band and the core electrons and is more attractive with increasing coverage.

We now examine the relation between the shift of the Kohn-Sham potential at the surface relative to the bulk, the initial-state surface $3d$ core-level shift, and the displacement of the center of gravity of the surface $4d$ band, ΔC_d . In Fig. 4 we show the spherically symmetric part of the surface potential shift $\Delta V(r) = V^{\text{surf}}(r) - V^{\text{bulk}}(r)$ together with $r^2 |R_{3d}(r)|^2$, and with $r^2 |R_{4d}(r)|^2$, where $R_{3d}(r)$ and $R_{4d}(r)$ are the radial solutions of the Schrödinger equation within the muffin-tin sphere. We see that $\Delta V(r)$ is almost constant up to ≈ 1.2 bohr away from the core. Yet, this is the region sampled by the $3d$ core electrons. Interestingly, the numerical values of the initial-state SCLS's are not merely correlated but are nearly equal to $-4\pi \int \Delta V(r) r^2 |R_{3d}(r)|^2 dr$.³⁵ This occurs because the $3d$ orbital is more tightly bound than the $4d$ orbital and $\Delta V(r)$ is approximately constant in the region in which the $3d$ orbital is localized, and the radial wave function is normalized. The potential shift is repulsive for those Rh surface atoms which are not bound to O (type A). Adsorption of oxygen induces large changes in the surface potential; increasing the O coverage leads to more attractive potentials at the surface, which in turn is felt by the core electrons and gives rise to the initial-state contribution to the SCLS's. The behavior of the potential shifts and the initial-state trend as coverage increases correlate with the calculated increase of the work function as a function of O coverage, which reflects an oxygen induced inward dipole moment, i.e., with the negative charge at the vacuum side of the surface.¹¹ Thus the gross behavior of the initial-state shifts reflects the electronegativity of oxygen. The Rh $3d$ binding energy increases by about 0.3 eV per bond to an oxygen adatom. At this point, it is worth clarifying our view regarding the origin of the initial-state shifts. Although we so far have focused solely on displacements induced by charge

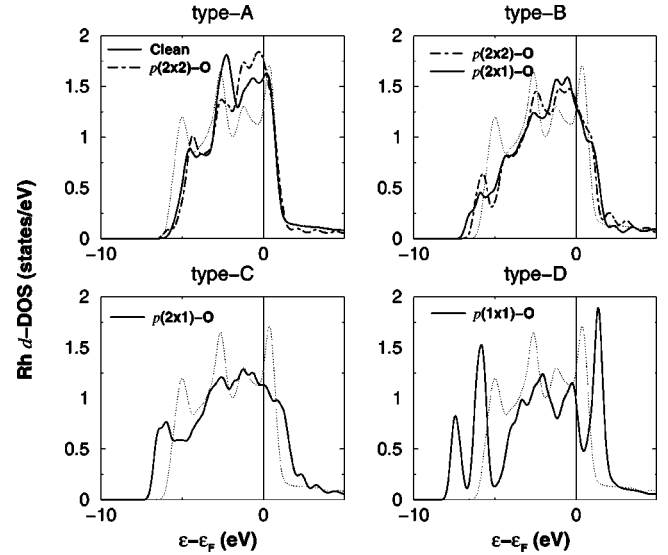


FIG. 5. Projected density of states per Rh atom onto the $4d$ orbitals for all surface atoms at the coverages considered (initial-state calculations). Type-A atoms are not bound to oxygen. B, C, and D are Rh atoms coordinated to one, two, or three O adatoms, respectively. The dotted lines correspond to Rh bulk.

transfer from the metal to the adsorbate, i.e., a partial ionization of surface atoms, we are by no means ruling out the possibility that there are also other non-negligible contributions such as charge redistribution or rehybridization effects. We note that a *clear* separation of these individual effects is not well defined.^{36,37}

The changes in the surface potential are reflected in the initial-state SCLS's and in the changes in the d band of surface atoms compared to bulk ones. Figure 5 displays the density of states per atom projected onto the d orbitals (d DOS), $N_d(\epsilon)$, for all surface and bulk atoms. For the clean surface and type-A atoms of the $p(2 \times 2)$ -O structure a narrower and displaced (towards lower binding energy) d DOS is clearly visible. In comparison with the type-A surface atoms, the d DOS for type-B, C, and D atoms is broader (relative to the bulk). Applied to these projected densities of states, we have calculated the shift in the center of gravity $\Delta C_d = -[\epsilon_d^{\text{surf}} - \epsilon_d^{\text{bulk}}]$ of the d DOS as a measure of the response of the d electrons to the surface potential shift. The center of gravity of the local density of states is given by $\epsilon_d = \mu_1 / \mu_0$, where $\mu_i = \int \epsilon^i N_d(\epsilon) d\epsilon$ is the i th moment of the d spectrum. The moment μ_0 gives the *total* number of d states in the d band.³⁸ The calculated ΔC_d 's between the bulk and surface d bands and the initial-state shifts are shown in Fig. 6 (top panel). These results show that the initial-states SCLS's and the shift in the center of gravity of the d DOS follow the same trend.³⁹

We have seen that the SCLS's nearly equal $-4\pi \int dr \Delta V(r) r^2 |R_{3d}(r)|^2$ given that the core orbitals are confined to a localized region around the nucleus where $\Delta V(r)$ has approximately a constant value. However, the $4d$ orbitals are quite broad and sample a potential shift little different from that sampled by the $3d$ orbitals (see Fig. 4).⁴⁰ Hence, one anticipates quantitative differences between both

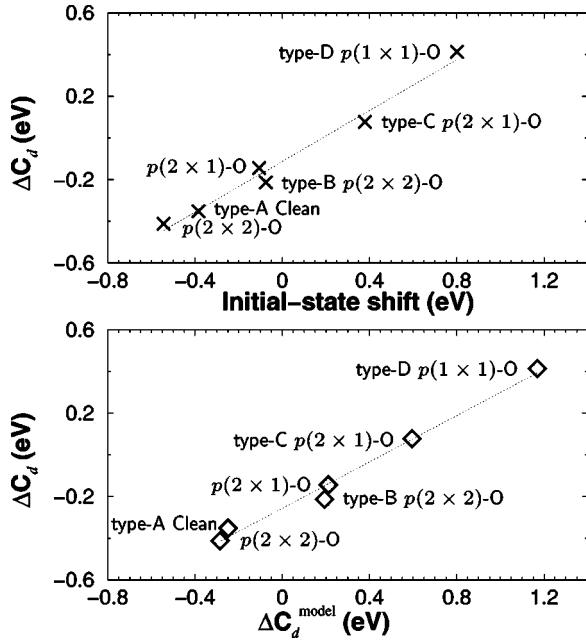


FIG. 6. Top panel: The calculated shift of the d -band center between the self-consistent bulk and surface d bands and the initial-state core-level shifts. Bottom panel: The calculated shift of the d -band center between the self-consistent bulk and surface d bands and the corresponding shift resulting from a simple rectangular d -DOS model as described in the text.

samplings of the perturbation $\Delta V(r)$, i.e., between the magnitude of the SCLS's and ΔC_d 's. The qualitative correlation between ΔC_d 's and initial-state shifts reflects that the shift of the d band and the SCLS's arise from the same oxygen induced surface potential shifts as experienced by the d states and core states, respectively.

After establishing the relation between the initial-state SCLS's and ΔC_d 's, it is important to recognize that the repulsive potential shift between surface and bulk atoms for late transition clean metal surfaces is assumed to occur primarily to conserve d charge,³⁵ defined as $f_d = \int \epsilon^\epsilon N_d(\epsilon) / \mu_0 d\epsilon$.⁴¹ We discuss here a model, in which the complex self-consistent d -band structure is mapped onto a simple rectangular d DOS of width W . Thus the density of states per atom will take the constant value $10/W$, because the d band must hold exactly ten electrons when it is full. For free Rh atoms the atomic configuration is d^8s^1 . Within this model the layerwise d -charge conservation condition $f_d = 8/10$ gives $C_d^{\text{model}} = -\frac{3}{10}W$ for each layer, where C_d^{model} is the position of the center of gravity of the rectangular d band of width W . We note that C_d^{model} lies in the middle of the rectangular band.

The presence of broken bonds at the clean surface leads to a narrowing of the local d -density of states and oxygen chemisorption to a broadening (see Fig. 5). From this simple model we can calculate the displacement of the center of gravity of the rectangular surface d DOS (relative to the bulk), $\Delta C_d^{\text{model}}$, that it is necessary to recover conservation of d -charge when the width is varied. The width of the model bulk band, W_{bulk} is calculated from $C_d^{\text{model}} = -\frac{3}{10}W$ consid-

TABLE II. The calculated d -band filling f_d in percent for the bulk and the (111) surface of Rh as function of the O coordination or type, given in parentheses (see Fig. 2).

Coverage	O coordination		f_d
Bulk			80%
Clean	0	(A)	80%
0.25	0	(A)	80%
	1	(B)	79%
0.50	1	(B)	79%
	2	(C)	77%
1.00	3	(D)	76%

ering that the positions of the center of gravity of the model bulk band and the actual self-consistent band coincide.

From the calculated mean-square deviation of the d DOS, $\mu_2/\mu_0 - (\mu_1/\mu_0)^2$, of both self-consistent surface and bulk d bands, we obtain the relative change of the bandwidth, ΔW . Therefore we assume that the variation of mean-square deviation between the self-consistent surface and bulk d bands and that between corresponding model d bands remains similar. For the model bands $W = [12(\mu_2/\mu_0 - (\mu_1/\mu_0)^2)]^{1/2}$.⁴² Having calculated the relative width changes ΔW , the conservation of d charge for a surface site, $C_d^{\text{model}} = -\frac{3}{10}W_{\text{bulk}}(1 + \Delta W)$, gives the displaced center of gravity of the model surface band. Further details can be found in Ref. 23.

Figure 6 (bottom panel) compares the calculated shifts of the d -band center between the self-consistent bulk and surface d bands and the corresponding $\Delta C_d^{\text{model}}$ shifts. The most striking feature to be noticed is the qualitative similar trends of $\Delta C_d^{\text{model}}$ and the initial-state SCLS's. Thus this simple model captures the contribution to the shifts arising from the oxygen induced surface d -band broadening. The difference between the initial-state shifts and $\Delta C_d^{\text{model}}$ varies between -100 and -400 meV, and it is larger for higher O coverages. We note that the model predicts a shift towards higher binding energies due to an O-induced broadening of the surface bandwidth in order to fulfill strict conservation of d charge. In Table II we give the calculated values for the d -band filling f_d in percent for the self-consistent d DOS of the bulk and the (111) surface of Rh as a function of the O coordination. It is seen that the conservation of d charge is *approximately* valid. However, assuming a strict conservation of d charge at high O coverages leads to larger positive shifts than the actual required if conservation of d charge holds *approximately*. Despite the simplicity of the model, an estimation of the initial-state values for the SCLS's assuming the core levels rigidly follow the $\Delta C_d^{\text{model}}$ displacements would be a reasonable approximation. Solving the problem self-consistently, however, ensures the inclusion of redistribution of valence charge at the surface and charge transfer from the metal surface to the oxygen adlayer, which are not captured by the simple model.

2. Final-state effects

In order to unambiguously interpret measured values of core-level shifts, it is necessary to consider the effect of the

screening of the core hole by the other electrons. The inclusion of these effects has been performed within the transition-state theory [see Eq. (1)], as described in Sec. III. The resulting full shifts are shown in Fig. 2 and listed in Table I. The final-state contributions to the shifts are explicitly shown in Fig. 3. We observe that the quasilinear correlation between SCLS's and coordination to O adatoms is robust with respect to differences between initial-state and transition-state theory calculations of the SCLS's. The magnitude of the screening contribution is small compared to that of the initial-state shift. This, however, does not mean that this term can be neglected since its magnitude amounts in some cases up to $\sim 15\%$ of the full shift, and in general tends to improve the agreement to the measured SCLS's. We note, however, that the *sign* of the initial-state and that of the full transition-state theory SCLS's is always the same; in general, even this does not hold necessarily.²¹ Thus final-state effects, while not insignificant, do not appear to be the dominant factor responsible for the Rh 3*d* SCLS's considered.

Looking into more detail at this contribution it is seen that it changes sign as the oxygen coverage increases (see Fig. 3). The sign change of the final-state contributions to the shifts can be qualitatively explained by tracing back to the oxygen induced changes in the surface electronic structure. It has been already mentioned that a negative final-state contribution to the SCLS's, as for the clean surface, means that a core hole in a surface atom is better screened than one in a bulk atom. This enhanced screening at the surface atom of a late transition metal is partially due to a better intra-atomic screening provided by the high-lying localized *d* states at the atom from which the core electron is emitted.²⁰ Comparing the projected densities of states per Rh atom onto the 4*d* orbitals for a bulk and surface atom at the clean Rh(111) surface, one observes the higher density of high-lying localized *d* states about the Fermi level (see Fig. 5). For the ad-layer systems, however, the screening at the surface becomes worse upon increasing O coverage. In fact, at a coverage of 1.0 ML it is positive and largest in magnitude (see Fig. 3). The screening of a Rh 3*d* core hole created at high oxygen covered surfaces is less efficient because of the oxygen induced decrease of *d* states about the Fermi level localized at the respective atom (see Fig. 5).

C. Experiment vs theory

The comparison of our experimental and theoretical results for the Rh 3*d* shifts of the surface layer atoms as a function of O coverage (see Fig. 2) indicates that there is no doubt that Rh atoms bonding to none, one, or two O atoms, can easily be distinguished by their 3*d* binding energies. On closer examination, however, there are some quantitative differences between calculated and measured values of the SCLS's. For the oxygen covered surfaces, the largest difference is ~ 0.10 eV for the type-C atoms, while for type-B atoms it is a factor of 2 smaller. Even if the agreement is good, we have to say that the small differences between experimental and theoretical results can also be due to the finite temperature of the measurements ($T=300$ K). It has been recently demonstrated that SCLS of the clean Rh(100) sur-

TABLE III. The Rh 3*d* surface core-level shifts (meV) of second substrate layer atoms of the clean and O-covered Rh(111) surfaces within the transition-state theory and from the initial-state model as a function of coverage. The third column shows the difference and gives the screening contribution to the shifts. For the 0.25- and 0.50-ML phases, from the two inequivalent second layer atoms, only the value which is non-negligible is listed (see text).

Coverage	Full calc.	Initial state	Final state
Clean	+67	+96	-29
0.25	-150	-164	+14
0.50	-155	-173	+18
1.00	-217	-216	~ 0

face decreases when the surface temperature increases, because of the expansion of the first interlayer distance.⁴³ Moreover, the fitting procedure strategy is completely independent of the theoretical results and assumes three distinguishable components in order to limit the number of free parameters. In order to unambiguously confirm the assignments, we have calculated the initial and final-state contributions to the Rh 3*d* SCLS's for all Rh atoms underneath the surface layer, i.e., of the second substrate layer (see Table III). The experimental positions of the Rh 3*d* levels (relative to bulk) as a function of O coverage up to 0.5 ML and the results of the full transition-state theory calculation for the shifts at the two outermost substrate layers are schematically compared in Fig. 7. The shift experienced by the 3*d* core levels of the second substrate layer atoms in the clean Rh(111) surface is one order of magnitude smaller than that of the surface atoms and remained experimentally unresolved. For the O-covered surfaces, there are two inequivalent Rh second layer atoms at both 0.25 and 0.50 ML coverages, respectively. Our results indicate that for each coverage only one kind has a sizable shift and the other coincides with the bulk peak. The corresponding non-negligible full shifts are -150 meV (0.25 ML) and -155 meV (0.50 ML) (see Table III). Although the magnitude of these shifts is sizable, they remain experimentally unresolved as they are superimposed to the measured type-B atoms surface peak. The calculated full shifts at the second substrate layer atoms of the $p(2\times 2)$ and $p(2\times 1)$ structures differ by only 65 and 39 meV from those of type-B Rh surface atoms at the same coverage, respectively (see Table I). Figure 7 clearly demonstrates that the experimental spectra resolve the main features of the oxygen induced shifts. In conclusion, the overall agreement between experimental and theoretical data is not only qualitatively very good but also quantitatively satisfactory. Although some minor discrepancies have arisen, it is clear that surface core-level spectroscopy in combination with calculations of the kind performed in this work offer the possibility of studying the local geometrical and electronic environment of metal atoms as a function of oxygen coverage. This will turn out to be relevant for identifying the chemical state of subsurface oxygen and oxide formation in the O/Rh(111) system.⁴⁴

Together with analyses of the Rh 3*d* shifts we have measured and calculated the O 1*s* shifts relative to the O 1*s* level

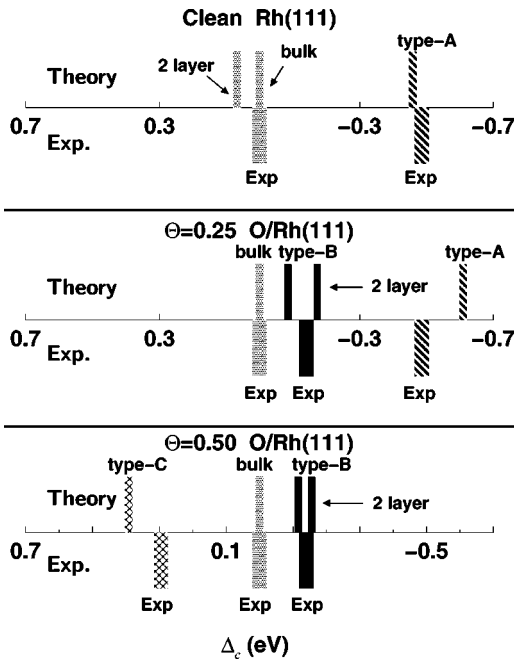


FIG. 7. The experimental positions of the Rh $3d$ surface levels relative to the bulk ones, for the clean and O-covered surfaces (Exp.), and the full transition-state theory calculation for the shifts at the surface and the layer beneath (Theory). For the second substrate layer atoms, only the shifts which are different from zero are shown (see text). The different patterns in the lower panels indicate the different experimental resolved positions as a function of coverage. In the upper panels, the labels indicate from which atoms the shifts originate and the lines which remained experimentally unresolved have the same pattern.

for the $p(2 \times 2)$ -O ($\Theta = 0.25$ ML) structure. The results are shown in Fig. 8. In contrast to the Rh $3d$ shifts, the O $1s$ spectra show only minor changes between the 0.25- and 0.50-ML structures. At 0.50 ML the calculated O $1s$ full shift, relative to O atoms at the 0.25-ML coverage, is -34 meV (initial state -10 meV), and the measured value is -110 ± 30 meV. The calculated evolution of the O $1s$ shift versus coverage shows that at 1.0 ML the full shift is $+237$ meV (initial state $+190$ meV). The initial-state trend can be understood by taking into consideration that as oxygen coverage increases ($\Theta > 0.5$ ML) the distance between similarly negatively charged O adatoms decreases and a repulsive interaction builds up. Reducing electron transfer is energetically favorable as it reduces the repulsion. Thus at high coverages O $1s$ levels are shifted towards higher binding energies. This positive shift correlates with the calculated coverage dependence of the work function, which rises linearly but reaches its saturation value at ≈ 0.75 ML. This behavior of the oxygen induced work-function changes is consistent with the decrease of the oxygen induced inward dipole moment per adatom as a consequence of the dipole-dipole interaction which gives rise to a depolarization with decreasing O-O distance.¹¹ The projected density of states onto the O $2p$ orbitals for atoms of the 0.25- and 1.0-ML overlayers are displayed in Fig. 9. The O $2p$ DOS at 1.0 ML clearly shows a splitting and subsequent downward shift of

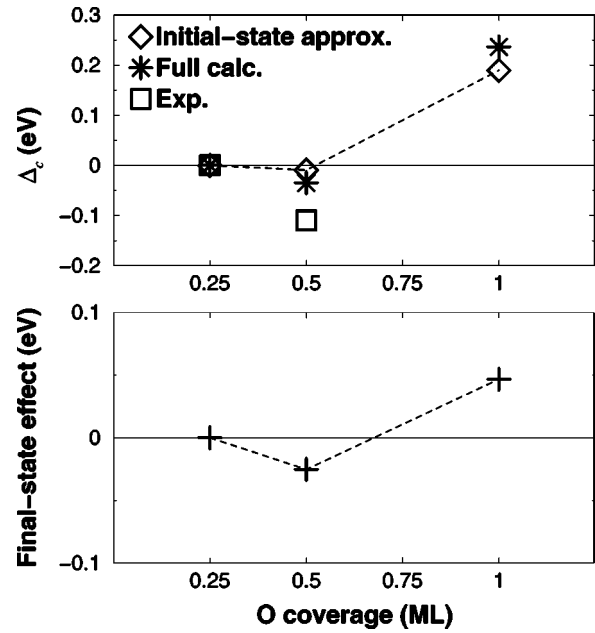


FIG. 8. Top panel: Initial-state and full transition-state theory calculation for the O $1s$ shifts for the $p(2 \times 2)$, $p(2 \times 1)$, and (1×1) -O phases on Rh(111) at coverages of $\Theta = 0.25, 0.5$, and 1.0 ML, respectively, relative to the lowest coverage phase. Comparison between calculated and measured values is shown for the $p(2 \times 1)$ -O phase. Lower panel: Calculated final-state contribution to the O $1s$ shifts.

the bonding states localized on the oxygen atoms due to O-O interactions. The magnitude of the screening contributions is small compared to that of the initial-state shift.

The comparison of core-level photoelectron spectroscopy measurements with a theoretical study of core-level shifts induced by chemisorption may also be a valuable tool to check for different possible adsorption geometries and analyze the chemical bonding in the stable adsorption sites (see, e.g., Refs. 15 and 18). The similarity of the O $1s$ binding

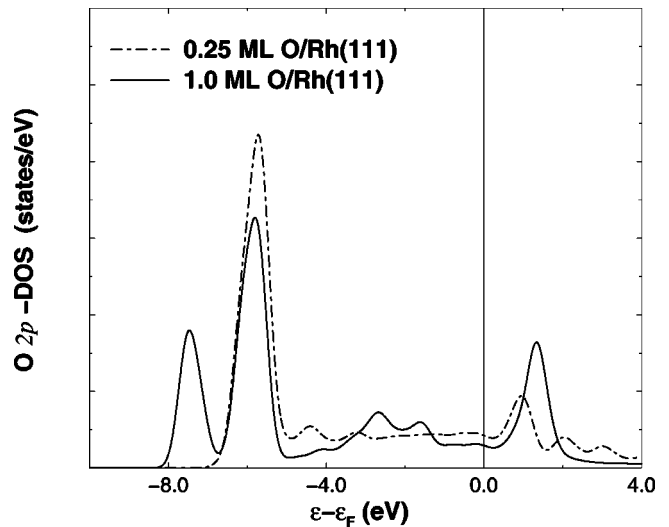


FIG. 9. Projected density of states per O atom onto the $2p$ orbitals for the $p(2 \times 2)$ and (1×1) -O phases on Rh(111).

energy for the lowest coverage $p(2\times 2)$ and $p(2\times 1)$ -O structures is consistent with the occupation of the same (fcc) adsorption sites. In seeking qualitative explanations for the stability of the fcc sites, we calculated the difference in O $1s$ binding energy between the fcc and the hcp sites at a coverage of 0.25 ML. A shift of 0.36 eV is obtained. The binding energy for fcc sites is shifted towards lower values. Final-state contributions to this difference are negligible (~ 0.01 eV). This shift can be correlated with the calculated larger work-function increase for fcc adsorption by ~ 0.1 eV. These results are consistent with an increased electrostatic repulsion at the stable fcc site, where a somewhat more negatively charged O is adsorbed. Thus O finds fcc hollows on Rh(111) favorable because of a stronger *ionic* bonding, which also seems to be the dominant factor stabilizing the on-surface sites upon subsurface oxygen formation.⁴⁴

V. SUMMARY

In summary, we have shown that the combination of experimental and theoretical determination of Rh $3d$ SCLS's is a valuable tool to study the effect of O chemisorption on Rh(111). SCLS's are sensitive not only to the presence of O on the surface but also to the detailed geometrical structure of the O overlayer. Interpretation of core-level shifts is more complicated than generally acknowledged since a number of effects contribute to an experimentally observed shift. Theory can help to disentangle these terms. In particular, the decomposition into initial- and final-state effects presented here indicates that the former appear to be the dominant factor influencing the oxygen induced Rh $3d$ SCLS's. We have demonstrated that the initial-state contributions to the Rh $3d$ SCLS's are accurately given by the average of the surface potential shift over the $3d$ orbitals, and that SCLS's and the surface d -band shift ΔC_d , which measures the response of the valence d electrons to the potential shift, follow the same trend. We have found a quasilinear correlation between the magnitude of the SCLS's and the coordination to O adatoms which is robust with respect to differences between initial-state and transition-state theory calculations of the shifts. Thus measured SCLS's do provide a qualitative measure of the changes in the Rh valence band upon O chemisorption (an initial-state effect). This is not a general conclusion.

The almost linear dependence of the SCLS's with the number of directly coordinated O atoms shows that Rh atoms bonding to none, one, or two O atoms can easily be distin-

guished by their $3d$ binding energies: The Rh $3d$ binding energy increases by about 0.3 eV per bond to an O adatom. This initial-state shift towards higher binding energies is oxygen induced and is precisely what is expected from the high electronegativity of oxygen adatoms. Assuming *strict* layerwise conservation of d charge and by mapping the self-consistent d DOS for Rh surface and bulk atoms onto rectangular model d bands with similar relative changes of the mean-square width as those of the actual d bands, we have calculated the displacement of the center of gravity of the model surface d bands, $\Delta C_d^{\text{model}}$, relative to the bulk. We have shown that d charge is approximately conserved for *real* self-consistent d bands and that the model captures the contributions to the shifts arising from the oxygen induced d -band broadening. Solving the more complex self-consistent problem ensures the inclusion of redistribution of valence charge at the surface and charge transfer from the metal surface to the oxygen adlayer.

The calculated work-function change as a function of coverage reflects an oxygen induced inward dipole layer which gives rise to a potential at the surface which is consistent with the calculated initial-state shifts. The O adatoms become depolarized with increasing O coverage, thereby decreasing the charge transfer. Consistently, our calculated O $1s$ level at $\Theta = 1.0$ ML (relative to the $\Theta = 0.25$ ML structure) shifts towards higher binding energy.

The magnitude of the final-state contributions to the Rh $3d$ SCLS's is small compared to the initial-state shifts and it changes from negative to positive with increasing O coverage. The sign change could be qualitatively explained by examining the oxygen induced changes in the surface electronic structure. The results support the importance of being able to quantify the differences in screening of the core hole for the unambiguously interpretation of measured shifts.

This study appears to provide an example of a *trend* and its interpretation, and we believe that surface core-level spectroscopy in combination with calculations of the kind performed in this work offer a tool to improve our understanding of the O-metal interaction in different chemical environments.

ACKNOWLEDGMENTS

We thank K. Reuter for useful discussions concerning the theoretical SCLS's analysis and P. Blaha for helpful comments on the FP-LAPW (WIEN) code.

¹See G. Comelli, V. R. Dhanak, M. Kiskinova, K. C. Prince, and R. Rosei, *Surf. Sci. Rep.* **32**, 165 (1998), and references therein.

²J. T. Grant and T. W. Haas, *Surf. Sci.* **21**, 70 (1970).

³D. G. Castner, B. A. Sexton, and G. A. Somorjai, *Surf. Sci.* **71**, 519 (1978); D. G. Castner and G. A. Somorjai, *ibid.* **83**, 60 (1979); D. G. Castner and G. A. Somorjai, *Appl. Surf. Sci.* **6**, 29 (1980).

⁴K. C. Wong, K. C. Hui, M. Y. Zhou, and K. A. R. Mitchell, *Surf. Sci.* **165**, L21 (1986).

⁵K. C. Wong, W. Liu, and K. A. R. Mitchell, *Surf. Sci.* **360**, 137 (1996).

⁶S. Schwegmann, H. Over, V. De Renzi, and G. Ertl, *Surf. Sci.* **375**, 91 (1997).

⁷S. Schwegmann and H. Over, *Surf. Sci.* **393**, 179 (1997); H. Xu and K. Y. S. Ng, *ibid.* **393**, 181 (1997).

⁸H. Xu and K. Y. S. Ng, *Surf. Sci.* **375**, 161 (1997).

⁹T. Greber, J. Wider, E. Wetli, and J. Osterwalder, *Phys. Rev. Lett.* **81**, 1654 (1998).

- ¹⁰D. Loffreda, D. Simon, and P. Sautet, *J. Chem. Phys.* **108**, 6447 (1998).
- ¹¹M. V. Ganduglia-Pirovano and M. Scheffler, *Phys. Rev. B* **59**, 15 533 (1999).
- ¹²K. D. Gibson, M. Viste, E. C. Sanchez, and S. J. Sibener, *J. Chem. Phys.* **110**, 2757 (1999).
- ¹³J. Wider, T. Greber, E. Wetli, T. J. Kreuzt, P. Schwaller, and J. Osterwalder, *Surf. Sci.* **417**, 301 (1998); **432**, 170 (1999).
- ¹⁴W. F. Egelhoff, *Surf. Sci. Rep.* **6**, 253 (1987).
- ¹⁵N. Martensson and N. Nilsson, in *High Resolution Core-Level Photoelectron Spectroscopy of Surfaces and Adsorbates*, edited by W. Eberhardt, Springer Series in Surface Science Vol. 35 (Springer-Verlag, Berlin, 1994), p. 65.
- ¹⁶D. Menzel, *Chemistry and Physics of Solid Surfaces*, edited by R. Vanselow (CRC Press, Boca Raton, FL, 1979), Vol. II, p. 227.
- ¹⁷D. Spajaard, C. Guillot, M. C. Desjonqueres, G. Treglia, and J. Lecante, *Surf. Sci. Rep.* **5**, 1 (1985).
- ¹⁸A. Baraldi, S. Lizzit, and G. Paolucci, *Surf. Sci. Lett.* **457**, L354 (2000).
- ¹⁹E. Pehlke and M. Scheffler, *Phys. Rev. Lett.* **71**, 2338 (1993).
- ²⁰M. Methfessel, D. Hennig, and M. Scheffler, *Surf. Rev. Lett.* **2**, 197 (1995).
- ²¹M. V. Ganduglia-Pirovano, J. Kudrnovský, and M. Scheffler, *Phys. Rev. Lett.* **78**, 1807 (1997).
- ²²K. Reuter (private communication).
- ²³S. Lizzit, A. Baraldi, A. Grosso, K. Reuter, M. V. Ganduglia-Pirovano, C. Stampfl, M. Scheffler, M. Stichler, C. Keller, W. Wurth, and D. Menzel, *Phys. Rev. B* (to be published).
- ²⁴A. Abrami *et al.*, *Rev. Sci. Instrum.* **66**, 1618 (1995).
- ²⁵A. Baraldi, M. Barnaba, B. Brena, D. Cocco, G. Comelli, S. Lizzit, G. Paolucci, and R. Rosei, *J. Electron Spectrosc. Relat. Phenom.* **76**, 145 (1995).
- ²⁶J. C. Slater, *Quantum Theory of Molecules and Solids* (McGraw-Hill, New York, 1974), Vol. 4, pp. 51-55; J. F. Janak, *Phys. Rev. B* **18**, 7165 (1978).
- ²⁷J. P. Perdew, J. A. Chevary, S. H. Vosko, K. A. Jackson, M. R. Pederson, D. J. Singh, and C. Fiolhais, *Phys. Rev. B* **46**, 6671 (1992).
- ²⁸P. Blaha, K. Schwarz, and J. Luitz, WIEN97, Vienna University of Technology, 1997. [Improved and updated Unix version of the original copyrighted WIEN code, which was published by P. Blaha, K. Schwarz, P. Sorantin, and S. B. Trickey, *Comput. Phys. Commun.* **59**, 399 (1990).]
- ²⁹M. Petersen, F. Wagner, L. Hufnagel, M. Scheffler, P. Blaha, and K. Schwarz, *Comput. Phys. Commun.* **126**, 294 (2000).
- ³⁰B. Kohler, S. Wilke, M. Scheffler, R. Kouba, and C. Ambrosch-Draxl, *Comput. Phys. Commun.* **94**, 31 (1996).
- ³¹S. Doniach and M. Šunjić, *J. Phys. C* **3**, 185 (1970).
- ³²J. N. Andersen, D. Hennig, E. Lundgren, M. Methfessel, R. Nyholm, and M. Scheffler, *Phys. Rev. B* **50**, 17 525 (1994).
- ³³J. N. Andersen, M. Qvarford, R. Nyholm, S. L. Sorensen, and C. Wigren, *Phys. Rev. Lett.* **67**, 2822 (1991).
- ³⁴M. Alden, H. L. Skriver, and B. Johansson, *Phys. Rev. Lett.* **71**, 2449 (1993); M. Alden, I. A. Abrikosov, B. Johansson, N. M. Rosengaard, and H. L. Skriver, *Phys. Rev. B* **50**, 5131 (1994).
- ³⁵M. V. Ganduglia-Pirovano, V. Natoli, M. H. Cohen, J. Kudrnovský, and I. Turek, *Phys. Rev. B* **54**, 8892 (1996).
- ³⁶J. Bormet, J. Neugebauer, and M. Scheffler, *Phys. Rev. B* **49**, 17 242 (1994).
- ³⁷M. Scheffler and C. Stampfl, in *Handbook of Surface Science*, edited by K. Horn and M. Scheffler (Elsevier Science, Amsterdam, 2000), Vol. 2, p. 286.
- ³⁸We calculate the d -DOS, $N_d(\epsilon)$, only inside the muffin-tin spheres of the FP-LAPW scheme. As can be seen in Fig. 4, the $4d$ orbital extends beyond the currently chosen sphere of 2.2 Bohr radius. Thus the calculated d -DOS contains fewer d states, and the number of total d states changes with the choice of sphere radius. The center of gravity ϵ_d , given by the ratio between first and zeroth moment of the d -DOS, changes by less than 20 meV for a 10% decrease in the muffin-tin radius. These variations are small compared to the overall trend of the calculated ΔC_d 's.
- ³⁹The upper integration limit for the calculation of the first moments of the density of states is not well defined. We have integrated all states up to $\epsilon_{\max} = (\epsilon - \epsilon_F) = 3.5$ eV. It is found that changes in ΔC_d are negligible (± 5 meV) when varying ϵ_{\max} to either 3.0 or 4.0 eV.
- ⁴⁰Note that in Fig. 4 only the radial solutions $r^2|R_{nl}(r)|^2$, $nl=3d$ and $4d$ within the muffin-tin sphere in the bulk are displayed. The purpose of the figure is to provide a qualitative understanding in the existence of a correlation between the responses of the core-electrons and of the d band to the surface perturbation $\Delta V(r)$. Corrections due to the details of the radial solutions within the muffin-tin sphere at the surface and in the bulk are to be considered for a more quantitative analysis.
- ⁴¹We note that f_d is defined as the ratio between the number of occupied states and the total number of states μ_0 and is practically independent of the choice of muffin-tin radius. As indicated in Ref. 39, we have integrated all states up to $\epsilon_{\max} = (\epsilon - \epsilon_F) = 3.5$ eV. It is found that changes in f_d are negligible (less than 0.1%) when varying ϵ_{\max} to either 3.0 or 4.0 eV.
- ⁴²D. Pettifor, *Bonding and Structure of Molecules and Solids* (Clarendon Press, Oxford, 1995).
- ⁴³A. Baraldi, G. Comelli, S. Lizzit, R. Rosei, and G. Paolucci, *Phys. Rev. B* **61**, 12 713 (2000).
- ⁴⁴M. V. Ganduglia-Pirovano and M. Scheffler (unpublished).